Thermodynamic Properties of the Redox Centers of Na^+-Translocating NADH:Quinone Oxidoreductase†

Alexander V. Bogachev,‡ Yulia V. Bertsova,‡ Dmitry A. Bloch,§ and Michael I. Verkhovsky*,§

Department of Molecular Energetics of Microorganisms, A. N. Belozersky Institute of Physico-Chemical Biology, Moscow State University, Moscow 119899, Russia, and Institute of Biotechnology, P.O. Box 65, Viikinkaari 1, University of Helsinki, 00014 Helsinki, Finland

Received November 28, 2005; Revised Manuscript Received January 23, 2006

ABSTRACT: Redox titration of all optically detectable prosthetic groups of Na^+-translocating NADH:quinone oxidoreductase (Na^+-NQR) at pH 7.5 showed that the functionally active enzyme possesses only three titratable flavin cofactors, one noncovalently bound FAD and two covalently bound FMN residues. All three flavins undergo different redox transitions during the function of the enzyme. The noncovalently bound FAD works as a "classical" two-electron carrier with a midpoint potential (E_m) of −200 mV. Each of the FMN residues is capable of only one-electron reduction: one from neutral flavosemiquinone to fully reduced flavin (E_m = 20 mV) and the other from oxidized flavin to flavosemiquinone anion (E_m = −150 mV). The lacking second half of the redox transitions for the FMNs cannot be reached under our experimental conditions and is most likely not employed in the catalytic cycle. Besides the flavins, a [2Fe-2S] cluster was shown to function in the enzyme as a one-electron carrier with an E_m of −270 mV. The midpoint potentials of all the redox transitions determined in the enzyme were found to be independent of Na^+ concentration. Even the components that exhibit very strong retardation in the rate of their reduction by NADH at low sodium concentrations experienced no change in the E_m values when the concentration of the coupling ion was changed 1000 times. On the basis of these data, plausible mechanisms for the translocation of transmembrane sodium ions by Na^+-NQR are discussed.

NADH:quinone oxidoreductases from the marine bacteria of the genus *Vibrio* form a family of primary redox-driven Na^+ pumps that generate transmembrane differences in electrochemical potentials of sodium ions ($\Delta\mu_{Na^+}$)[1] (*1*−*4*). The efficiency of Na^+ translocation by the enzyme was shown to be 1 Na^+/e^- (*5*).

The Na^+-translocating NADH:quinone oxidoreductase (Na^+-NQR) consists of six subunits (NqrA−F) (*6*) that correspond to the six genes of the *nqr* operon (*7*, *8*). Subunit NqrF possesses binding motifs for NADH, FAD, and an iron−sulfur center and mediates the NADH dehydrogenase activity of the enzyme (*7*, *9*, *10*). The presence of the iron−sulfur center in Na^+-NQR was confirmed by EPR spectroscopy that showed a [2Fe-2S]-type cluster (*11*−*13*). Na^+-NQR isolated from different bacterial species also contains tightly bound ubiquinone-8 and noncovalently bound FAD with a molar ratio of ca. 1:1 (*11*, *13*, *14*). In addition, Na^+-NQR bears two covalently bound FMN residues that are attached by phosphoester bonds to threonine residues in subunits NqrB and NqrC (*3*, *14*−*16*). Recently, a noncovalently bound riboflavin was also reported in Na^+-NQR (*17*). Note that it has been generally accepted that living organisms use riboflavin only as a precursor for FAD and FMN synthesis (*18*), and thus, Na^+-NQR is so far the only enzyme in which riboflavin has been proposed to be a cofactor. However, there are no data about the subunit to which Na^+-NQR riboflavin could bind. Moreover, there is a possibility that Na^+-NQR contains only three flavins, whereas the observed riboflavin is a hydrolysis product of FMN residues (*4*).

The kinetics of reduction of Na^+-NQR by NADH displays three distinct phases corresponding to reduction of three different flavin species, as shown by studies using stopped-flow optical spectroscopy (*12*, *19*). This reaction can be dissected into two parts with respect to the coupling site location. The first part (before the coupling site) is the sodium-independent fast reduction of FAD to $FADH_2$ at the NADH dehydrogenating domain of Na^+-NQR. The second part (after the coupling site) consists of the two slower phases that are strongly dependent on the sodium concentration. It was shown that the two sodium-dependent phases reflect the reduction of the neutral flavosemiquinone to the fully reduced flavin and that of the oxidized flavin to the anionic flavosemiquinone, respectively. Therefore, we have proposed that at least one of these one-electron transitions is coupled to the transmembrane sodium translocation by Na^+-NQR

† This work was supported by the Russian Foundation for Basic Research (Project 04-04-48101), the Academy of Finland (Projects 200726 and 44895), Biocentrum Helsinki, and the Sigrid Jusélius Foundation.

* To whom correspondence should be addressed. Phone: +358 9 191 58005. Fax: +358 9 191 58 001. E-mail: michael.verkhovsky@helsinki.fi.

‡ Moscow State University.

§ University of Helsinki.

[1] Abbreviations: DM, dodecyl maltoside; EPR, electron paramagnetic resonance; Fl, oxidized flavin; FlH_2, reduced flavin; $FlH^•$, neutral flavosemiquinone; $Fl^{•-}$, anionic flavosemiquinone; LDAO, lauryldimethylamine *N*-oxide; Na^+-NQR, Na^+-translocating NADH:quinone oxidoreductase; $\Delta\mu_{Na^+}$, transmembrane difference of Na^+ electrochemical potentials.

10.1021/bi052422x CCC: $33.50
Published on Web 02/15/2006

(*4*, *19*). The question of the redox center through which electron transfer to the Na^+ translocation is coupled could be resolved by equilibrium redox titration. The mechanism of energy conversion between the redox transitions and the transmembrane translocation of a sodium ion is still unknown for Na^+-NQR. Generally, redox−electrochemical coupling takes place if, for example, the electrostatic field formed upon reduction of a Na^+-NQR cofactor is compensated by the capture of the sodium ion from the cytoplasmic side of the membrane. The subsequent oxidation of this cofactor has to be accompanied by the ejection of the cation from the other side of the membrane (*4*, *7*). If this mechanism is the case, the redox potential of at least one enzyme cofactor should depend on the Na^+ concentration. Thus, redox titration of Na^+-NQR at different concentrations of Na^+ seems promising for understanding the catalytic mechanism of the enzyme and localization of the coupling site.

In this work, redox titration of all the optically detectable Na^+-NQR cofactors has been accomplished. We have found the amazing result that under equilibrium conditions all the determined redox transitions in the enzyme are sodium-independent.

MATERIALS AND METHODS

Bacterial Strains and Growth Conditions. *Escherichia coli* (XL1-Blue) and *Vibrio cholerae* cells were grown in LB medium at 37 °C. Antibiotics that were used were 100 μg/mL ampicillin and 10 μg/mL tetracycline for *E. coli* and 150 μg/mL ampicillin and 50 μg/mL streptomycin for *V. cholerae*. *Vibrio harveyi* cells were grown as described previously (*14*).

Cloning and Expression of the nqrABCDEF Operon from V. harveyi. The *nqr*ABCDEF operon of *V. harveyi* with its own promoter was amplified from genomic DNA using PCR with "Long Reading" polymerase ("Sileks") and primers dirA (5′-AAACAGCATCAAAACCGGACACT) and revF (5′-GCCATAGATTCAATCACTTGCGG). The amplified fragment (~6 kb) was cloned into the pGEM-T vector, resulting in the pLN52 plasmid. This plasmid was used as a template for the next PCR with another pair of primers, nqrAdir (5′-CAAGTGCccATgGTTACAATA) and nqrF_rev (5′-CACTTGCGGGaATTcACC), containing *Nco*I and *Eco*RI sites, respectively. The PCR product obtained was cloned into the pBAD/*Myc*-HisC vector between its *Nco*I and *Eco*RI sites, resulting in pBAD/nqr4 plasmid (bearing the *nqr* operon under control of an arabinose promoter with a six-histidine tag fused in frame to the C-terminus of the *nqr*F gene product). This plasmid was digested by *Kpn*I and *Ssp*I restrictases, and a ~2.6 kb band containing a part of the *nqr* operon with *nqr*F fused with the six-histidine tag was inserted into the pLN52 plasmid between the *Kpn*I and *Sal*I sites in place of the original part of the *nqr* operon. This procedure resulted in cloning of the complete *nqr* operon with the six-histidine-tagged *nqr*F gene under control of the *nqr* promoter (pLN52-his1 plasmid).

The pLN52-his1 plasmid was incorporated into *V. cholerae* 0395N1-*toxT*::*lacZ* Δ*nqr* cells (*13*) using electroporation (*20*).

Recombinant His-tagged Na^+-NQR was purified using affinity chromatography. Membranes from cells of *V. cholerae* 0395N1-*tox*T::*lac*Z Δ*nqr*/pLN52-his1 were suspended in solution A [350 mM KCl, 5 mM imidazole, and 20 mM Tris-HCl (pH 8.0)], solubilized with 1% DM, and centrifuged at 200000*g* for 60 min. The supernatant was loaded onto a Ni−NTA column equilibrated with solution B (solution A containing 0.05% DM). The column was successively washed with solution B containing 10 and 20 mM imidazole. Na^+-NQR was then eluted from the column with solution B containing 100 mM imidazole. The enzyme obtained was concentrated and frozen at −80 °C until it was used. This purification yielded Na^+-NQR preparations with specific NADH-dehydrogenase and Q_1-reductase activities of 92 and 48 μmol of NADH consumed per minute per milligram of protein, respectively.

Na^+-NQR from V. harveyi cells was purified as described previously (*12*) with minor modifications. For protein solubilization, 2.5% Liponox-DCH was used instead of LDAO and all purification steps were carried out in the presence of 0.2% Liponox-DCH instead of LDAO or DM. This procedure yielded Na^+-NQR preparations with specific NADH-dehydrogenase and Q_1-reductase activities of 48 and 26 μmol of NADH consumed per minute per milligram of protein, respectively.

Spectroelectrochemistry. Spectropotentiometric redox titration of Na^+-NQR was carried out as described using an optically transparent, thin layer electrode (OTTLE) cell (*21*−*23*). Potentials within the range of −400 to 140 mV versus the SHE were set with ±20 mV steps during both oxidative and reductive titration using a PAR263A potentiostat (Princeton Applied Research). Optical absorption spectra were recorded in the spectral range of 350−770 nm at a succession of redox potentials. At each potential step, the onset of equilibrium on the working electrode was determined, as the changes in the cell current and optical density at 460 nm became no longer significant (20−35 min/step). The titrations were performed at 21 °C. The setup was PC-controlled in a fully automated regime using Titrator version 2.41 (2004−2005) developed by N. Belevich (Helsinki, Finland).

Two layers of gold minigrid (300 lpi, each layer with a 70% transmittance, Buckbee-Mears, Europe GmbH) served as the working electrode. The minigrid surface was prepared as described in ref *13*. A Pt wire immersed in 3 M KCl and a saturated Ag/AgCl half-cell served as the counter electrode and reference electrode, respectively.

To accelerate the redox equilibrium between the working electrode surface and the solubilized enzyme molecules, hexaammineruthenium (E_m = 50 mV), pentaaminechlororuthenium (E_m = −130 mV), and methyl viologen (E_m = −455 mV) were used as redox mediators (the E_m values and stabilities of the mediators when present in a mixture were checked in situ using cyclic voltammetry). No optical contribution from hexaammineruthenium or pentaaminechlororuthenium (ABCR GmbH & Co.) was detected in the spectral range that was studied. The contribution from methyl viologen was taken into account during the data analysis.

For the spectroelectrochemical experiments, Na^+-NQR samples were washed with buffer C [150 mM KCl, 20 mM HEPES-Tris (pH 7.5), 0.05% DM, 50 μM methyl viologen, 400 μM pentaaminechlororuthenium(III) chloride, and 200 μM hexaammineruthenium(III) chloride] and concentrated on spinnable filters (Millipore) up to 50 μM Na^+-NQR; the mixture (~40 μL) was used to fill the OTTLE cell. All redox potentials that are quoted refer to the SHE.

Redox Titration of Na^+-NQR Using Lactate/Pyruvate Redox Buffer. Na^+-NQR samples (~3 mg/mL) in 20 mM HEPES-Tris (pH 7.5), 50 mM KCl, and 0.05% DM were titrated under strictly anaerobic conditions by varying the lactate/pyruvate ratio (10 mM pyruvate and 0.1−10 mM L-lactate) in the presence of NAD^+ (5 mM) and lactate dehydrogenase (1 unit). In these experiments, the Tris salts of NAD^+, lactate, and pyruvate were used. In the absence of added Na^+, the background sodium concentration in the mixture was 20 μM. Anaerobic samples were prepared using a vacuum line with several cycles of degassing and flushing with argon gas.

Spectra of the kinetic phases of the Na^+-NQR reduction by NADH and spectra of glucose oxidase were obtained as described previously (*19*). To estimate the quantity of Na^+-NQR cofactors during redox titration of the enzyme, the following extinction coefficients were used: $\epsilon_{450} = 12.3$ mM^{-1} cm^{-1} (Fl → FlH_2), $\epsilon_{570} = 3.9$ mM^{-1} cm^{-1} ($FlH^\bullet$ → FlH_2), and $\epsilon_{450} = 10.8$ mM^{-1} cm^{-1} (Fl → $Fl^{\bullet-}$) (*24*, *25*).

Noncovalently bound flavins were extracted from Na^+-NQR as described previously (*14*). Extracted flavins were separated by reverse-phase HPLC using a Prontosil 120-5C18AQ column (dimensions of 75 mm × 2 mm). A linear gradient of methanol [total sweep from 10 to 70% (v/v), 25 min] in 5 mM MES-Tris (pH 6.0) with a flow rate of 0.1 mL/min was used. Flavins were detected at 360 nm. The retention times for FAD, FMN, and riboflavin standards were 12.4, 14.0, and 15.1 min, respectively.

NADH-dehydrogenase and Q_1-reductase activities of Na^+-NQR were measured as described previously (*12*).

The protein content was determined by the bicinchoninic acid method using bovine serum albumin as a standard. The sodium concentration was measured by flame photometry. All chemicals were analytical grade and were obtained from Sigma-Aldrich unless otherwise stated.

RESULTS

The *nqr* operon was cloned from genomic DNA of *V. harveyi*. By using this construct, a six-histidine tag was fused with the C-terminus of the NqrF subunit, which is similar to the approach described in ref *13*. The tagged *V. harveyi nqr* operon was then heterologously expressed in the *V. cholerae* Δ*nqr* strain.

In this study, two types of enzyme preparation were used: (i) NQR, the Na^+-NQR partially purified by a conventional technique from the wild-type *V. harveyi* cells, and (ii) NQR-his, the recombinant enzyme highly purified by affinity chromatography.

Spectropotentiometric Redox Titration of Na^+-NQR. The redox titration of the enzyme was performed by the spectroelectrochemical approach at potentials between −400 and 140 mV with steps of 20 mV in both the oxidative and reductive direction. The spectral changes in the protein upon reductive and oxidative titration were practically identical, and the hysteresis at any step was less than 10 mV. For further analysis, the spectra obtained under the same potentials in the oxidative and reductive directions were averaged.

Figure 1 shows a typical set of spectral changes of NQR-his during redox titration in the presence of 50 mM Na^+. At each step, reduction caused a decrease in the absorbance of the sample, with the exception that there was a small positive absorbance change upon reduction at very low redox potentials. The latter was due to methyl viologen, whose spectral changes were subtracted prior to further analysis. Examination of the redox potentials outside the defined region did not show any additional spectral changes within the enzyme (data not shown).

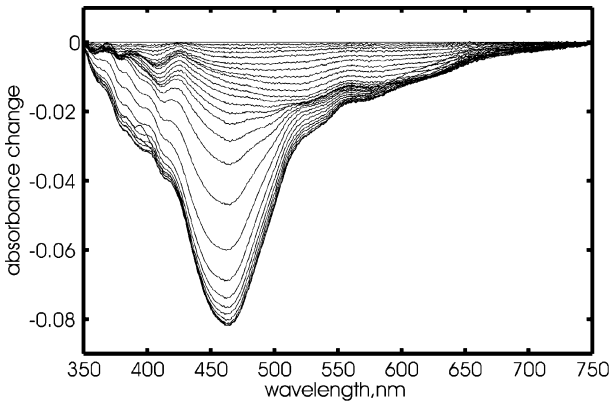

FIGURE 1: Difference spectra (reduced minus oxidized) of NQR-his obtained during spectroelectrochemical titration at redox potentials from 140 to −400 mV with −20 mV steps. The spectrum at 140 mV was used as the reference. Reduction caused a decrease in the absorbance of the protein over the whole range of potentials. The optical path length was 0.6 mm and the bulk volume 40 μL. For conditions, see Materials and Methods.

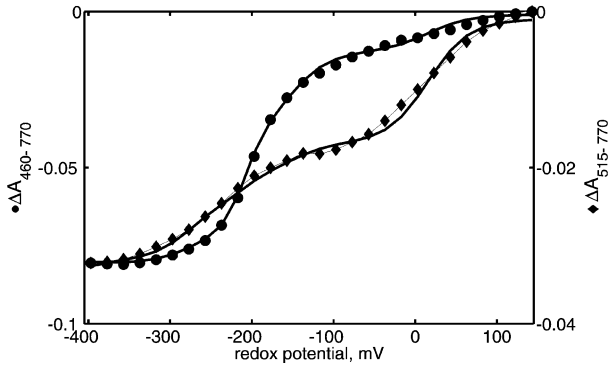

FIGURE 2: Redox titration of NQR-his monitored at 460 (●) and 515 nm (♦). The absorbance at 770 nm was taken as a reference. Lines representing the theoretical titration curves at the selected wavelengths were plotted using the fit parameters as in Figure 3. Conditions were as described in the legend of Figure 1.

Analysis of the first derivative of the optical density measured at different wavelengths along the redox potential axis brought out four maxima corresponding to the four redox components in the data set. One of the peaks was sharper and taller than the others and could be described well as a two-electron component. At the same time, the three other components were typical one-electron transitions.

The dependence of the optical density at two different wavelengths on the redox potential is illustrated in Figure 2. The data for 460 nm, where oxidized flavins have their maximal absorbance, can be roughly described by two redox transitions: (i) a two-electron transition ($n = 2$) with an E_m of ca. −200 mV and (ii) a one-electron transition ($n = 1$) with an E_m of ca. −150 mV (a minor contribution of two transitions with E_m values of 10 and −270 mV are also observed; see below). The data for 515 nm, where the major contribution is expected from the reduction of $FlH^\bullet$ and an Fe−S cluster, could be described by two major one-electron

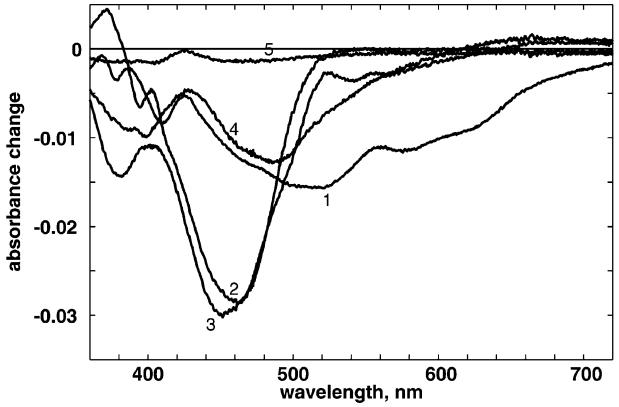

FIGURE 3: Spectral components of Na^+-NQR (NQR-his preparation) obtained from redox titration. Lines 1−4 represent the spectral components: line 1, $E_m = 16$ mV and $n = 1$; line 2, $E_m = -155$ and $n = 1$; line 3, $E_m = -209$ mV and $n = 2$; line 4, $E_m = -272$ mV and $n = 1$; and line 5, the residuals of the data fit (eq 1). Conditions were as described in the legend of Figure 1.

transitions with E_m values of ca. −270 and 10 mV, respectively.

Thus, we made a global fitting of the complete data set assuming that the system contains one two-electron and three one-electron transitions. The redox potential dependence of the absorbance changes at any wavelength can be presented as

$$A_\lambda(E_h) = \sum_{i=1}^{4} \epsilon_\lambda^i \times \frac{10^{(n^i/60)(E_h - E_m^i)}}{10^{(n^i/60)(E_h - E_m^i)} + 1} \qquad (1)$$

where A_λ is the absorbance at a particular wavelength λ, ϵ_λ^i is the extinction of the ith redox center at this wavelength, E_h is the ambient redox potential in millivolts, E_m^i is the midpoint redox potential of the ith redox center in millivolts, and n^i is number of electrons required for reduction of the ith redox center. Fitting the model (eq 1) to the data set presented as a surface $A_\lambda^{obs}(E_h)$ gave us four ϵ_λ^i spectral components and four values of their E_m^i midpoint potentials ($i = 1$, 2, 3, and 4).

The results of the fit are plotted in Figure 3 (lines 1−4). It is noteworthy that the constant term of the fit reflecting changes which are not included in the spectral components (Figure 3, line 5) is negligible compared to the components themselves. Thus, the four components found entirely represent the whole visible spectral change of the enzyme detected within the potential range that was studied. This is also illustrated in Figure 2 where the fitting results are replotted as the theoretical titration curves at 460 and 515 nm (solid lines). Note that the curves fit well to the data that are plotted.

Assignment of the Spectral Components of Na^+-NQR. The component with the highest potential ($E_m = 16$ mV, $n = 1$, Figure 4A, solid line) is characterized by minima at 510, 575, and 625 nm. This spectrum is similar to the spectrum that was obtained by a study of the kinetics of reduction of Na^+-NQR by NADH (Figure 4A, dashed line) and was assigned to the Na^+-dependent reduction of neutral flavosemiquinone to fully reduced flavin (*4*, *19*). Thus, we attribute this spectral component to the $FlH^\bullet \rightarrow FlH_2$ transition.

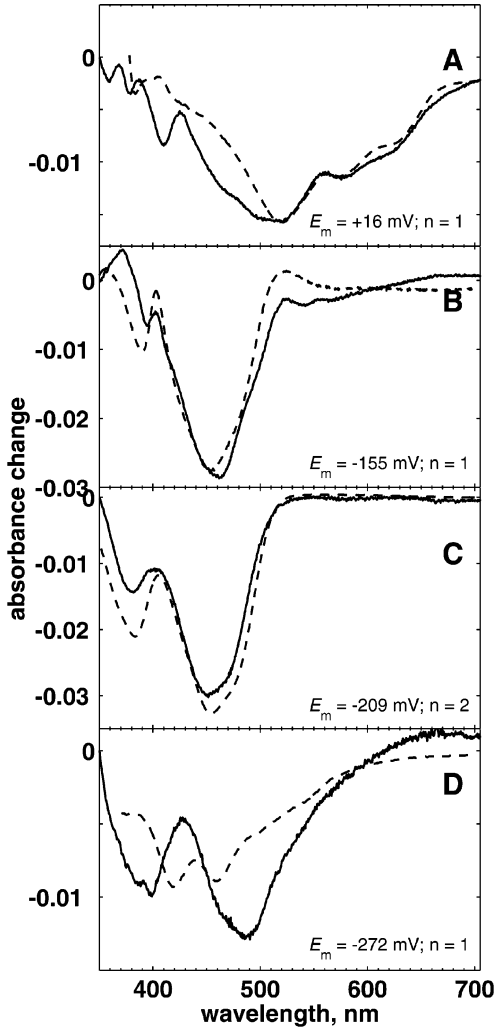

FIGURE 4: Absorption spectra of components obtained from redox titration of Na^+-NQR (NQR-his preparation) in comparison with model spectra of flavins and the [2Fe-2S] cluster. (A) Spectrum of the $E_m = 16$ mV ($n = 1$) component (—) compared with the spectrum of one-electron reduction of neutral flavosemiquinone in Na^+-NQR (*18*) (- - -). (B) Spectrum of the $E_m = -155$ mV ($n = 1$) component (—) compared with the spectrum of one-electron reduction of FAD in glucose oxidase with the formation of anionic flavosemiquinone (*18*) (- - -). (C) Spectrum of the $E_m = -209$ mV ($n = 2$) component (—) compared with the spectrum of two-electron reduction of glucose oxidase (*18*) (- - -). (D) Spectrum of the $E_m = -272$ mV ($n = 1$) component (—) compared with spectrum of reduction of spinach ferredoxin (- - -).

The next component ($E_m = -155$ mV, $n = 1$, Figure 4B, solid line) has a major trough at 458 nm and minor peaks at 370, 400, and 515 nm. The spectrum is close to one found as the slowest kinetic component during the enzyme reduction by NADH (not shown) and assigned to the reduction of oxidized flavin to flavosemiquinone anion. For demonstration, Figure 4B also shows a model spectrum of the $Fl \rightarrow Fl^{\bullet-}$ transition (dashed line) obtained by the anaerobic photoreduction of the glucose oxidase under alkaline conditions (*4*, *19*). The spectra are very similar, and we attribute the component with an E_m of −155 mV to the $Fl \rightarrow Fl^{\bullet-}$ transition in Na^+-NQR.

The fitting procedure gave us one two-electron component. Figure 4C shows the spectrum of this component (solid line) together with the spectrum of the $Fl \rightarrow FlH_2$ transition obtained by the two-electron reduction of glucose oxidase (dashed line). These two spectra are also very similar to the

Table 1: Midpoint Redox Potentials (in millivolts) of Na^+-NQR Cofactors at pH 7.5[a]

	NQR-his	NQR		
transition	50 mM Na^+	50 mM Na^+	50 μM Na^+	50 mM Na^+ and 200 μM NAD^+
$FlH^\bullet \rightarrow FlH_2$	16	25	10	23
$Fl \rightarrow Fl^{\bullet -}$	−155	−133	−161	−136
$Fl \rightarrow FlH_2$	−209 ($n = 2$)	−182 ($n = 2$)	−207 ($n = 2$)	−183 ($n = 2$)
$[2Fe\text{-}2S]^{2+} \rightarrow [2Fe\text{-}2S]^+$	−272	−267	−272	−307

[a] The number of electrons transferred is 1 ($n = 1$) for all transitions unless otherwise stated. The potentials refer to the SHE.

spectrum of the sodium-independent fast phase of the reduction of the enzyme by NADH, which we assigned to the two-electron reduction of a flavin (*18*). Therefore, we consider the component with an E_m of −209 mV ($n = 2$) to be a two-electron reduction of oxidized flavin ($Fl \rightarrow FlH_2$).

The lowest-potential component ($E_m = -272$ mV, $n = 1$) of the Na^+-NQR titration is shown in Figure 4D (solid line). The spectrum reveals two troughs at 395 and 480 nm and significant changes in the long wavelength region. It is most likely that the component represents a redox transition of the [2Fe-2S] cluster, because its redox properties are very similar to those of this Na^+-NQR cofactor ($E_m = -267$ mV, $n = 1$), as determined using the EPR technique (*12*). However, the spectrum of this component significantly differs from the model redox difference spectrum of a [2Fe-2S] cluster obtained using spinach ferredoxin (Figure 4D, dashed line). It is important that the component spectrum have a little in common with any spectra of flavin species, and its extinction is far too weak for the identification of this low-potential component as an additional "fourth" flavin cofactor.

The relative quantity of the flavin cofactors can be estimated using the extinction coefficients for different redox transitions of FAD in glucose oxidase (*19*). In the set of data in Figure 1, which we decompose into different components (Figure 4), the $Fl \rightarrow FlH_2$, $Fl \rightarrow Fl^{\bullet -}$, and $FlH^\bullet \rightarrow FlH_2$ transitions are present at 49, 43, and 42 μM, respectively, which is rather close to the expected 1:1:1 stoichiometry (a minor deviation from the expected stoichiometry can be explained by somewhat different molar extinctions of the flavin species in Na^+-NQR and glucose oxidase). Thus, the redox titration of Na^+-NQR in the presence of 50 mM Na^+ demonstrates four redox transitions of four enzyme cofactors: three flavins and one Fe−S cluster.

Besides that of the recombinant NQR-his enzyme, we also performed redox titration of wild-type NQR isolated from the *V. harveyi* cells by the conventional method (*12*). The titration yielded redox components practically identical to those for the His-tagged enzyme (see Table 1), except that in the wild-type NQR two minor additional components due to the presence of cytochromes *b* and *c* were also detected (data not shown; the latter was obviously due to the impurity of the NQR preparation compared to NQR-his).

Effect of Sodium on the Midpoint Redox Potentials of Na^+-NQR Cofactors. The main aim of this work was the determination of the dependence of the E_m values of all cofactors on the sodium concentration. This knowledge would let us define the steps in the catalytic cycle that are thermodynamically coupled to the translocation of sodium ions. To find the maximum effect, the experiment was performed in sodium-free medium (containing 40−60 μM Na^+ as an impurity). However, as can be seen from Table 1, the results of such measurements were not much different from those of the Na^+-NQR titration at 1000 times higher sodium concentrations. We conclude that the midpoint redox potential of all the redox components tested is practically sodium-independent.

To check that sodium dependence does not appear upon the binding of the natural electron donor NADH, we also carried out the electrochemical redox titration of Na^+-NQR in the presence of 200 μM NAD^+ and again did not find any shifts in E_m values (see Table 1).

The expected effect of sodium on the E_m of Na^+-NQR cofactors was also tested by the equilibrium perturbation method. For that purpose, the enzyme was poised at different redox potentials (−220, −190, and −160 mV) set by the lactate/pyruvate pair in the presence of NAD^+ and lactate dehydrogenase in the anaerobic sodium-free medium. Then NaCl was anaerobically added to a final concentration of 50 mM. We expected that if the midpoint potential of any of the cofactors were dependent on sodium concentration, the addition of this cation at certain potentials would significantly shift the equilibrium and change the spectrum of the protein. However, we were not able to discern any spectral change upon addition of NaCl (data not shown). This result also confirms the lack of the direct thermodynamic coupling between the electron affinity of optically detectable Na^+-NQR cofactors and sodium binding by this enzyme.

Flavin Content in Na^+-NQR. It was proposed earlier that Na^+-NQR contains four different flavins: one noncovalently bound FAD, two covalently bound FMN residues, and one noncovalently bound riboflavin (*10*, *17*). However, our data on the kinetics of the reduction of the enzyme by NADH (*19*) and especially the thermodynamic properties of Na^+-NQR (this paper) strongly show that there are only three flavin cofactors in the functionally active enzyme. Thus, to resolve these contradictions, we tried to reinvestigate the flavin content in Na^+-NQR.

The denaturation of NQR-his by trifluoroacetic acid followed by the separation of two fractions by sedimentation revealed 6.0 and 6.2 nmol of extractable and nonextractable flavin/mg of protein, respectively. This result shows that almost equal quantities of covalently and noncovalently bound flavin are present in the enzyme, which is in accordance with the data obtained previously with NQR (*14*).

Ultraviolet excitation of the electrophoresis gels of NQR or NQR-his preparations showed two fluorescent bands corresponding to NqrB and NqrC (data not shown). The data indicate the presence of two covalently bound flavins in Na^+-NQR, which is also in good agreement with earlier results (*3*, *16*).

Taking into account the equal quantities of covalently and noncovalently bound flavins, one could have concluded that Na^+-NQR also contained two noncovalently bound flavins and, therefore, four flavin cofactors in the enzyme as a whole.

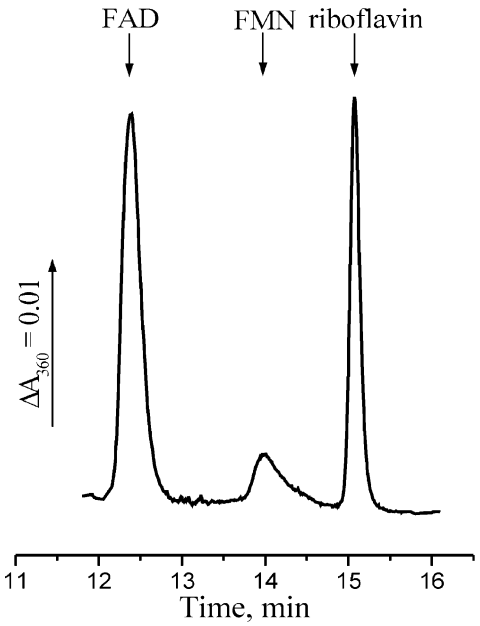

FIGURE 5: HPLC separation of the soluble flavin components extracted from Na^+-NQR (NQR-his preparation) after denaturation by trifluoroacetic acid. The quantities of FAD, FMN, and riboflavin were estimated to be 3.9, 0.67, and 2.0 nmol/mg of protein, respectively.

Indeed, the HPLC analysis of the trifluoroacetic acid extractable flavin fraction demonstrated the presence of riboflavin (Figure 5); this result was in full agreement with data reported previously (*10*, *17*). However, all tested Na^+-NQR preparations contained a much smaller quantity of riboflavin in comparison with FAD and also contain some quantity of FMN. In the example presented in Figure 5, the quantities are 2.0, 3.9, and 0.67 nmol of riboflavin, FAD, and FMN/mg of protein, respectively. In different preparations, the riboflavin:FAD ratio varied from 0.4 to 0.6. This value is surprisingly low compared to the expected ratio of 1:1. It is very likely that riboflavin and FMN found after acid extraction in the solution are the result of partial hydrolysis of the phosphoester bond of covalently bound FMN. In this case, extractable flavin consists of ~0.5 mol of riboflavin and 1 mol of FAD and gives 1.5 mol of flavin/mol of enzyme. The bound fraction would represent 2 mol of bound FMN residues minus 0.5 mol of hydrolyzed riboflavin which is also 1.5 mol of flavin/mol of enzyme. Such a result gives the apparent 1:1 ratio of bound and extractable flavins and explains completely the data set that was obtained.

DISCUSSION

In this work, we have performed redox titration of all the redox cofactors of Na^+-NQR that have absorbance in the visible spectral region: three flavins and one Fe−S cluster. The data obtained are very unusual. Surprisingly, all three flavins in Na^+-NQR undergo different redox transitions during the function of the enzyme. One of them works as a "classical" two-electron carrier, although the two others are capable of only a single one-electron reduction step. This conclusion agrees well with our earlier kinetic analysis of reduction of Na^+-NQR by NADH and EPR study of the enzyme (*18*). The one-electron transitions that we were able to observe were the $Fl \rightarrow Fl^{\bullet -}$ and $FlH^{\bullet} \rightarrow FlH_2$ transitions.

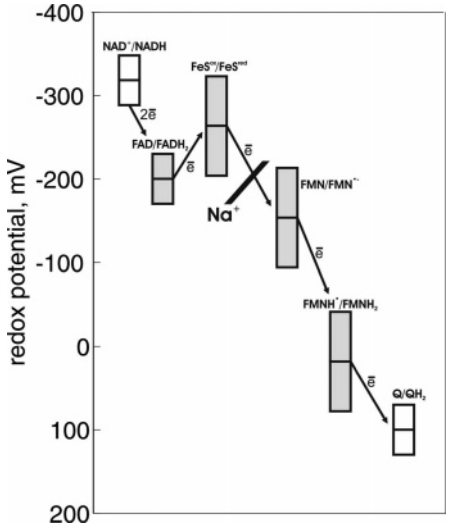

FIGURE 6: Scheme of the redox transitions of Na^+-NQR cofactors and possible sequence of electron transfer from NADH to ubiquinone.

Interestingly, the second half of both reactions ($Fl^{\bullet -} \rightarrow FlH_2$ and $Fl \rightarrow FlH^{\bullet}$, respectively) was never reached within the whole range of redox potentials that was studied. This finding agreed with previous EPR data which show the presence of the neutral flavosemiquinone in the completely oxidized enzyme and anionic flavosemiquinone in the fully reduced enzyme (*19*, *26*). To the best of our knowledge, this is the first demonstration that two one-electron transitions of flavin reduction in an enzyme can be so strongly energetically separated.

These results together with our previous data (*4*) let us assign the $Fl \rightarrow FlH_2$ transition with an E_m of −200 mV to the reduction of noncovalently bound FAD in the NADH-dehydrogenase domain of Na^+-NQR located in the NqrF subunit. The two one-electron transitions ($FlH^{\bullet} \rightarrow FlH_2$ with an E_m of 20 mV and $Fl \rightarrow Fl^{\bullet -}$ with an E_m of −150 mV) can be assigned to the reduction of two covalently bound FMN residues located in subunits NqrB and NqrC.

Summarizing sequence analysis of the Na^+-NQR subunits (*7*, *9*), kinetics of the enzyme reduction by NADH (*19*), and the thermodynamic properties of its cofactors (this work), we suggest a plausible scheme of electron transport within Na^+-NQR (Figure 6).

The C-terminal domain of the Na^+-NQR NqrF subunit is homologous to ferredoxin:$NADP^+$ oxidoreductases of the FNR family; it contains NADH and FAD binding sites (*7*, *9*). The N-terminal domain of NqrF resembles ferredoxins bearing a [2Fe-2S] cluster. Thus, NqrF is a polypeptide that combines NADH:ferredoxin oxidoreductase and a ferredoxin (*9*). Therefore, it seems obvious that at the beginning of the catalytic cycle two electrons from NADH are transferred to the noncovalently bound FAD. Then the electrons are apparently uncoupled, resulting in a FAD semiquinone and a reduced [2Fe-2S] cluster. The electron from the iron−sulfur cluster can be further transferred to covalently bound FMN residues and finally to ubiquinone. On the basis of the results of our redox titration, we assume that the electron from the iron−sulfur cluster is transferred to the FMN, producing $Fl^{\bullet -}$, and then to the $FlH^{\bullet}$, producing $FMNH_2$ (see Figure 6).

The kinetics of the reduction of Na^+-NQR by NADH studied earlier clearly shows two major components (*12*, *19*).

The first component was interpreted as the two-electron flavin reduction, its rate being essentially independent of sodium concentration. This sodium-independent component possibly includes the electron transfer from $FADH_2$ to the [2Fe-2S] cluster. However, with respect to the thermodynamic instability of FAD semiquinone (in redox titration this cofactor behaves like a pure two-electron mediator) and the lower E_m of the [2Fe-2S] cluster compared to that of the FAD/$FADH_2$ couple, this transition is energetically unfavorable. Thus, the steady-state [2Fe-2S] reduction takes place in only a small fraction of the enzyme and could not be detected.

The second component of the reduction of Na^+-NQR by NADH was interpreted as two sequential steps of one-electron reduction of two different flavin cofactors (the same way that we describe it in this paper). The rate of the second component was strongly increased in the presence of sodium ions. This is why we have assumed that one of latter transitions could be coupled to the transmembrane Na^+ translocation (*4*, *12*, *19*). Formally, such an assumption requires that the midpoint redox potential of a coupled transition be dependent on sodium concentration, and in a trivial case, it should increase by 60 mV per decade of sodium concentration. However, as we have demonstrated here, there is no such dependence for any of the Na^+-NQR cofactors. It is possible that the Na^+ concentration of 50 μM in the samples as a background contaminant was already too high to observe any sodium dependence of E_m values. However, this assumption would work out only if the sodium binding constant (K_s) is much lower than 50 μM. Such a high affinity is hardly probable because of the value of K_M^{app} of *V. harveyi* Na^+-NQR for Na^+ of 3 mM (*12*). Generally, of course, $K_M \neq K_s$, but in this case, the difference between the two constants seems to be too large. Note that *V. harveyi* is a marine bacterium, and in vivo, Na^+-NQR translocates Na^+ out of the cells against 0.5 M sodium normally present in seawater. If the "resting" $K_s \ll 50$ μM, the enzyme should be capable of shifting this value by more than 10^5 times during the catalytic cycle, which is not very likely.

Thus, our surprising results raise the question of how the mechanism of coupling of electron transfer to ion translocation and formation of $\Delta\mu_{Na^+}$ can be built so that the sodium affinity does not depend on electron affinity and vice versa.

There are several ways to answer such a question.

(1) We cannot completely exclude the existence of some invisible component, which has no changes in its absorbance in the visible spectral region but can have the expected sodium dependence of E_m. For example, we know that the enzyme contains a bound ubiquinone. However, ubiquinone itself is unlikely to be such a coupling cofactor because it serves as the final acceptor of electrons from Na^+-NQR, and we earlier demonstrated (*19*) that the coupling site is located in the scheme of the reaction between FAD and two FMNs. However, the possibility of the mediation of electron transfer by the sodium-dependent invisible and yet unknown cofactor still formally remains.

(2) An alternative explanation for the absence of any Na^+ dependence of midpoint redox potentials of Na^+-NQR cofactors is also possible. For example, one of the redox transitions that we followed in this work is coupled to both the binding of sodium to the enzyme from the cytoplasmic side and the release of another Na^+ from the periplasmic side. The oxidation of this cofactor would be coupled to translocation of the sodium ion from the cytoplasmic side to the periplasmic side of the enzyme. Such a mechanism does not lead to any sodium dependence of the midpoint redox potential(s), because reduction and oxidation do not change the amount of sodium ions bound to the enzyme.

(3) There is another possibility that Na^+-NQR is working not as a thermodynamic but rather as a kinetic machine. In this case, the sodium dependence of electron affinity of some Na^+-NQR cofactor arises during the catalytic cycle only as a result of consequent and ordered events. In other words, this sodium dependence is carried out only at a fixed stage of the catalytic cycle, which is not accessible under thermodynamic equilibrium conditions.

Further experiments are required to distinguish between the proposed alternatives for the mechanism of the coupling of sodium ion translocation to the electron transfer reactions in Na^+-NQR.

ACKNOWLEDGMENT

We thank Prof. M. Wikström and Prof. A. A. Konstantinov for helpful discussions, Dr. C. C. Häse for providing us with *V. cholerae* strains, and Dr. N. Belevich for providing us with software for the electrochemical setup. We are cordially indebted to Dr. Kai Vuorilehto for his assistance with the cyclic voltammetry experiments.

REFERENCES

1. Tokuda, H., and Unemoto, T. (1981) A respiration-dependent primary sodium extrusion system functioning at alkaline pH in the marine bacterium *Vibrio alginolyticus*, *Biochem. Biophys. Res. Commun. 102*, 265−271.
2. Tokuda, H., and Unemoto, T. (1982) Characterization of the respiration-dependent Na^+ pump in the marine bacterium *Vibrio alginolyticus*, *J. Biol. Chem. 257*, 10007−10014.
3. Hayashi, M., Nakayama, Y., Yasui, M., Maeda, M., Furuishi, K., and Unemoto, T. (2001) FMN is covalently attached to a threonine residue in the NqrB and NqrC subunits of Na^+-translocating NADH-quinone reductase from *Vibrio alginolyticus*, *FEBS Lett. 488*, 5−8.
4. Bogachev, A. V., and Verkhovsky, M. I. (2005) Na^+-translocating NADH:quinone oxidoreductase: Progress achieved and prospects of investigations, *Biochemistry (Moscow) 70*, 143−149.
5. Bogachev, A. V., Murtazina, R. A., and Skulachev, V. P. (1997) The Na^+/e^- stoichiometry of the Na^+-motive NADH:quinone oxidoreductase in *Vibrio alginolyticus*, *FEBS Lett. 409*, 475−477.
6. Nakayama, Y., Hayashi, M., and Unemoto, T. (1998) Identification of six subunits constituting Na^+-translocating NADH-quinone reductase from the marine *Vibrio alginolyticus*, *FEBS Lett. 422*, 240−242.
7. Rich, P. R., Meunier, B., and Ward, F. B. (1995) Predicted structure and possible ionmotive mechanism of the sodium-linked NADH-ubiquinone oxidoreductase of *Vibrio alginolyticus*, *FEBS Lett. 375*, 5−10.
8. Hayashi, M., Hirai, K., and Unemoto, T. (1995) Sequencing and the alignment of structural genes in the *nqr* operon encoding the Na^+-translocating NADH-quinone reductase from *Vibrio alginolyticus*, *FEBS Lett. 363*, 75−77.
9. Turk, K., Puhar, A., Neese, F., Bill, E., Fritz, G., and Steuber, J. (2004) NADH oxidation by the Na^+-translocating NADH:quinone oxidoreductase from *Vibrio cholerae*: Functional role of the NqrF subunit, *J. Biol. Chem. 279*, 21349−21355.
10. Barquera, B., Nilges, M. J., Morgan, J. E., Ramirez-Silva, L., Zhou, W., and Gennis, R. B. (2004) Mutagenesis study of the 2Fe-2S center and the FAD binding site of the Na^+-translocating NADH: ubiquinone oxidoreductase from *Vibrio cholerae*, *Biochemistry 43*, 12322−12330.

11. Pfenninger-Li, X. D. A. (1996) NADH:ubiquinone oxidoreductase of *Vibrio alginolyticus*: Purification, properties, and reconstitution of the Na^+ pump, *Biochemistry 35*, 6233−6242.
12. Bogachev, A. V., Bertsova, Y. V., Barquera, B., and Verkhovsky, M. I. (2001) Sodium-dependent steps in the redox reactions of the Na^+-motive NADH:quinone oxidoreductase from *Vibrio harveyi*, *Biochemistry 40*, 7318−7323.
13. Barquera, B., Hellwig, P., Zhou, W., Morgan, J. E., Häse, C. C., Gosink, K. K., Nilges, M., Bruesehoff, P. J., Roth, A., Lancaster, C. R., and Gennis, R. B. (2002) Purification and characterization of the recombinant Na^+-translocating NADH:quinone oxidoreductase from *Vibrio cholerae*, *Biochemistry 41*, 3781−3789.
14. Zhou, W., Bertsova, Y. V., Feng, B., Tsatsos, P., Verkhovskaya, M. L., Gennis, R. B., Bogachev, A. V., and Barquera, B. (1999) Sequencing and preliminary characterization of the Na^+-translocating NADH:ubiquinone oxidoreductase from *Vibrio harveyi*, *Biochemistry 38*, 16246−16252.
15. Nakayama, Y., Yasui, M., Sugahara, K., Hayashi, M., and Unemoto, T. (2000) Covalently bound flavin in the NqrB and NqrC subunits of Na^+-translocating NADH-quinone reductase from *Vibrio alginolyticus*, *FEBS Lett. 474*, 165−168.
16. Hayashi, M., Nakayama, Y., and Unemoto, T. (2001) Recent progress in the Na^+-translocating NADH-quinone reductase from the marine *Vibrio alginolyticus*, *Biochim. Biophys. Acta 1505*, 37−44.
17. Barquera, B., Zhou, W., Morgan, J. E., and Gennis, R. B. (2002) Riboflavin is a component of the Na^+-pumping NADH-quinone oxidoreductase from *Vibrio cholerae*, *Proc. Natl. Acad. Sci. U.S.A. 99*, 10322−10324.
18. Massey, V. (2000) The chemical and biological versatility of riboflavin, *Biochem. Soc. Trans. 28*, 283−296.
19. Bogachev, A. V., Bertsova, Y. V., Ruuge, E. K., Wikström, M., and Verkhovsky, M. I. (2002) Kinetics of the spectral changes during reduction of the Na^+-motive NADH:quinone oxidoreductase from *Vibrio harveyi*, *Biochim. Biophys. Acta 1556*, 113−120.
20. Barquera, B., Häse, C. C., and Gennis, R. B. (2001) Expression and mutagenesis of the NqrC subunit of the NQR respiratory Na^+ pump from *Vibrio cholerae* with covalently attached FMN, *FEBS Lett. 492*, 45−49.
21. Collins, M. J., Arciero, D. M., and Hooper, A. B. (1993) Optical spectropotentiometric resolution of the hemes of hydroxylamine oxidoreductase. Heme quantitation and pH dependence of E_m, *J. Biol. Chem. 268*, 14655−14662.
22. Ellis, W. R., Jr., Wang, H., Blair, D. F., Gray, H. B., and Chan, S. I. (1986) Spectroelectrochemical study of the cytochrome *a* site in carbon monoxide inhibited cytochrome *c* oxidase, *Biochemistry 25*, 161−167.
23. Arciero, D. M., Hooper, A. B., and Collins, M. J. (1994) Low volume spectroelectrochemistry: An anaerobic optically transparent thin layer electrode cell and a potentiostat/UV−Vis spectrophotometer interface for computer-controlled data collection, *J. Electroanal. Chem. 371*, 277−281.
24. Massey, V., and Palmer, G. (1966) On the existence of spectrally distinct classes of flavoprotein semiquinones. A new method for the quantitative production of flavoprotein semiquinones, *Biochemistry 5*, 3181−3189.
25. Stankovich, M. T., Schopfer, L. M., and Massey, V. (1978) Determination of glucose oxidase oxidation−reduction potentials and the oxygen reactivity of fully reduced and semiquinoid forms, *J. Biol. Chem. 253*, 4971−4979.
26. Barquera, B., Morgan, J. E., Lukoyanov, D., Scholes, C. P., Gennis, R. B., and Nilges, M. J. (2003) X- and W-band EPR and Q-band ENDOR studies of the flavin radical in the Na^+-translocating NADH:quinone oxidoreductase from *Vibrio cholerae*, *J. Am. Chem. Soc. 125*, 265−275.

BI052422X